

“Restoration” of Glutathione Transferase Activity By Single-site Mutation of The Yeast Prion Protein Ure2

Zai-Rong Zhang^{1,2}, Ming Bai¹, Xin-Yu Wang^{1,3}, Jun-Mei Zhou¹ and Sarah Perrett^{1*}

¹National Laboratory of Biomacromolecules, Institute of Biophysics, Chinese Academy of Sciences, 15 Datun Road, Chaoyang District, Beijing, 100101, China

²Graduate University of Chinese Academy of Sciences, 19 Yuquan Road, Shijingshan District, Beijing, 100049, China

³Department of Biophysics, Institute of Physics, Nankai University, 94 Weijin Road, Tianjin, 300071, China

Received 11 July 2008;
received in revised form
19 August 2008;
accepted 16 September 2008
Available online
27 September 2008

The yeast prion Ure2p is composed of an N-terminal prion domain, and a C-terminal globular domain, which shows similarity to glutathione transferases (GSTs) in both sequence and structure. Ure2p protects *Saccharomyces cerevisiae* cells from heavy metal ion and oxidant toxicity. Ure2p shows glutathione-dependent peroxidase (GPx) activity, which is often an adjunct activity of GSTs, but wild-type Ure2p shows no detectable GST activity toward the standard substrate 1-chloro-2,4-dinitrobenzene (CDNB). The structural basis for the substrate specificity of Ure2p enzymatic activity is an interesting problem that is fundamental to understanding the *in vivo* roles of Ure2p and its relationship to the GST structural family. The critical catalytic residue in the other known GSTs is Ser, Tyr or Cys. Here, we demonstrate that residue N124 is important for the GPx activity of Ure2p, and a wild-type level of activity is maintained in N124S, but not in N124Y/C. Interestingly, we found that the single-site mutations A122C and N124A/V (but not N124S/Y/C) “restore” the GST activity of Ure2p toward CDNB, while causing a substantial reduction in GPx activity. The steady-state kinetics for the GST activity of A122C appears to follow a ping-pong mechanism. In contrast, the GST activity of 124-site mutants shows a sequential mechanism, as is observed for the native GPx activity of Ure2p, and typical GST enzymes. These findings shed light on the evolutionary relationship of Ure2p with other GST family members, and contribute to our understanding of catalytic promiscuity and divergent evolution.

© 2008 Elsevier Ltd. All rights reserved.

Keywords: amyloid; Ure2p; glutathione S-transferase; protein engineering; enzyme

Edited by J. Weissman

Introduction

The glutathione transferases (GSTs) are a large versatile family of enzymes with a number of functions, particularly related to cellular

detoxification.^{1–5} In general, GSTs catalyze the conjugation of reduced glutathione (GSH) to toxic hydrophobic compounds containing an electrophilic carbon, nitrogen or sulfur atom in order to reduce their toxicity. In addition, GSTs bind a broad range of ligands and carry out a wide range of other functions. Some GSTs have functions overlapping with those of glutathione-dependent peroxidase (GPx) enzymes, indicating their role in metabolism of endogenous compounds such as peroxide and other products of oxidative stress. As a result, GSTs are associated with resistance to xenobiotics, drugs, insecticides, herbicides and antitumor drugs. GSTs are soluble dimeric proteins with a relatively conserved N-terminal thioredoxin-like domain bearing a $\beta\alpha\beta\alpha\beta\alpha$ topology that is responsible for GSH binding (the G-site), and a more variable C-terminal domain, which contains a pocket for binding a hydrophobic co-substrate (the H-site). This canonical GST fold is observed extensively in nature, sometimes showing different

*Corresponding author. E-mail address: sarah.perrett@iname.com.

Present address: Ming Bai, Department of Medicine, Harvard Medical School, and Division of Rheumatology, Immunology & Allergy, Brigham and Women’s Hospital, Boston, MA 02115, USA.

Abbreviations used: A122C-ox, Ure2p mutant A122C purified in the absence of DTT; CDNB, 1-chloro-2,4-dinitrobenzene; CHP, cumene hydroperoxide; GPx, glutathione-dependent peroxidase; GST, glutathione S-transferase; GSH, reduced glutathione; Ure2p-CTD, Ure2p C-terminal domain (residues 105–354); ThT, thioflavin T; WT, wild type.

functions not associated with GST, such as in bacterial stringent starvation protein A (SspA), the intracellular chloride ion channel (CLIC1), and the yeast prion Ure2p.¹⁻⁵

Ure2p is the protein determinant of the *Saccharomyces cerevisiae* prion [URE3].⁶ Analogous to the mammalian prion, the heritable [URE3] phenotype is conveyed by a structural change in Ure2p to an aggregated form.⁷ Ure2p is composed of a disordered protease-sensitive N-terminal domain and a compact globular domain whose structure has been determined in both apo and GSH-bound forms.⁸⁻¹⁰ The N-terminal approximately 90 amino acids are responsible for the conversion of Ure2p to the prion form *in vivo* and the formation of amyloid-like fibrils *in vitro*.^{7,11-13} Ure2p is involved in the regulation of nitrogen metabolism,¹⁴ and resistance to heavy metal, xenobiotic and oxidative stress¹⁵ in *S. cerevisiae*. The nitrogen metabolism regulation

function involves interaction of the C-terminal domain of Ure2p with the transcription factor Gln3p,¹⁶ and this function is lost when soluble Ure2p is converted to the aggregated form,⁷ although GPx activity is retained.^{15,17} Ure2p has a low level of sequence similarity with plant, insect and mammalian GSTs.¹⁶ The crystal structure of the C-terminal domain of Ure2p⁸⁻¹⁰ and the characterization of glutathione peroxidase activity of Ure2p¹⁷ confirm the classification of Ure2p as a glutathione transferase. However, efforts have failed so far to detect typical GST activity of Ure2p using widely used GST substrates, such as 1-chloro-2,4-dinitrobenzene (CDNB).^{15,16,18,19} Therefore, the evolutionary relationship between Ure2p and the GST family remains unclear. This study focuses on the GPx and GST activities of Ure2p mutants, in order to illuminate the role of the ancient GST fold in defining the enzymatic activity of Ure2p.

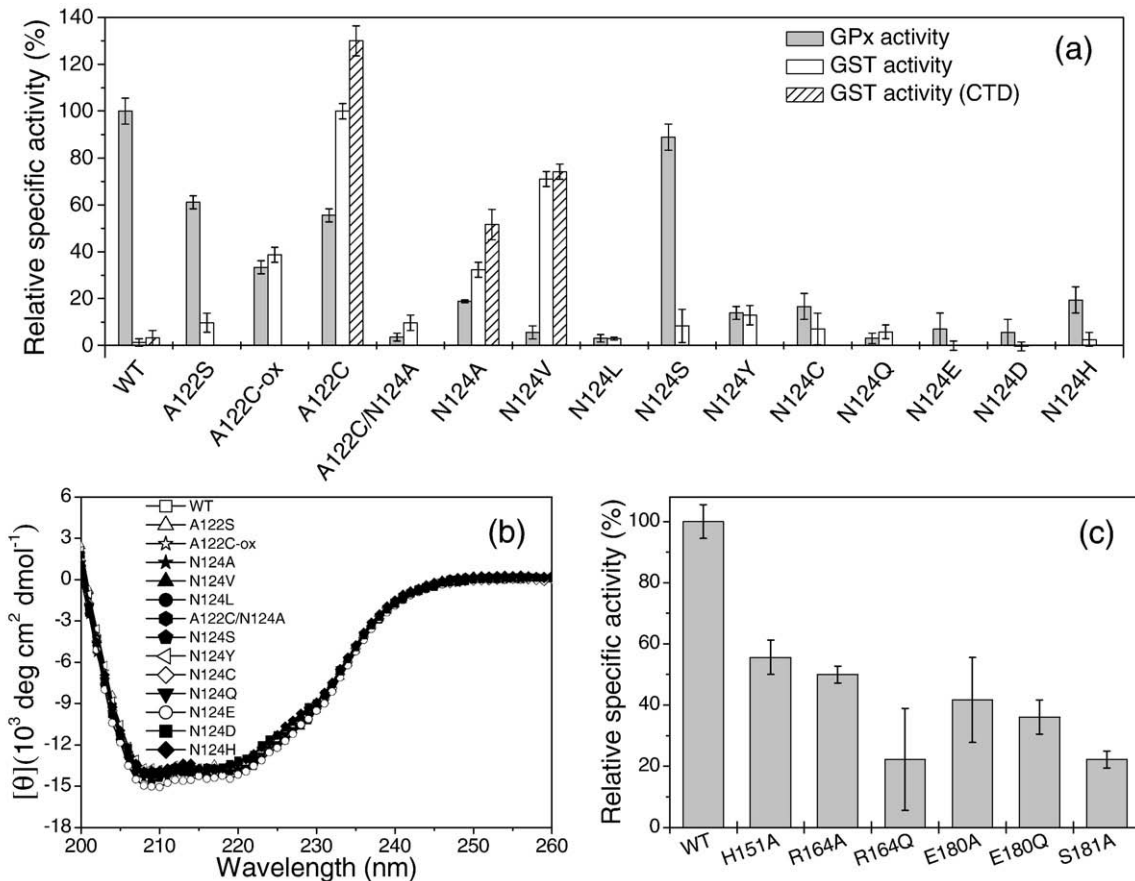


Fig. 1. (a) Effect of mutation of residue Ala122 and Asn124 on the GPx activity (filled bars) and GST activity (empty bars) of full-length Ure2p. The GPx activity of WT and the GST activity of A122C purified in the presence of DTT were defined as 100%. (A122C purified in the absence of DTT is denoted as A122C-ox.) The GST activity for the Ure2p C-terminal domain (CTD) is also shown for WT and the GST-active mutants A122C, N124A and N124V (hatched bars). The reaction conditions were 25 °C in 100 mM sodium phosphate buffer, pH 7.5 containing 1 mM GSH; with 1.2 mM CHP for GPx activity or 1 mM CDNB for GST activity. The protein concentrations were between 2 μM and 5 μM . The error bars represent the standard error of the mean of at least three repeated measurements. (b) Circular dichroism spectra of 122-site and 124-site mutants of full-length Ure2p indicates no change in native secondary structure. The Ure2p-CTD mutants displayed in panel a also showed no change in CD spectra (data not shown). (c) Comparison of GPx activity of other G-site mutants of Ure2p. The GST activity was also tested for these mutants, but negligible activity was observed (data not shown). The protein concentrations were between 1.0 μM and 3.0 μM . Other details were as in a.

Results

Identification of key amino acid residues involved in the GPx activity of Ure2p

The crystal structure of the Ure2p functional region in complex with GSH and related substrate analogs suggests that Asn124 may interact directly with the thiol group of GSH and therefore this residue may have a key role in the enzymatic activity of Ure2p.¹⁰ Therefore, we mutated Asn124 and measured the GPx activity of the mutants. When Asn124 was mutated to Ala, Val, Leu, Tyr, Cys, Gln, Glu, Asp or His, the GPx activity was lowered radically (Fig. 1a). The far-UV circular dichroism spectra showed no change (Fig. 1b), indicating that none of these mutants disrupts the secondary structure of the protein. The low level of activity of these 124-site mutants indicates that Asn124 has an important role in the GPx activity of Ure2p and, correspondingly, is likely to be important for protection against oxidative stress in yeast. An interesting finding is that the N124S mutant shows a level of activity similar to that of the wild type (WT) (Fig. 1a). The substitution of Asn by Ser may allow the enzyme to work in a similar way in the activation of the substrate GSH. Consistent with this, Ser has this role in a number of GST enzymes.³

Inspection of the crystal structure of the C-terminal domain of Ure2p¹⁰ suggests that Ala122 is close to the thiol group of GSH bound in the active site, and so we mutated this residue to Ser and Cys. A122S and A122C showed a similar reduction in GPx activity compared to WT, suggesting that the presence of Ala at site 122 allows better substrate alignment for GPx activity (Fig. 1a).

Several other residues, including His151, Arg164, Glu180, and Ser181, have also been suggested to be involved in GSH binding to Ure2p.¹⁰ Our data show that mutation of all these residues to Ala (or Gln) results in lower activity than WT Ure2p in the standard GPx activity assay (Fig. 1c), suggesting that these residues indeed contribute to substrate binding. However, the effects were less pronounced than mutation of residue Asn124.

Introduction of GST activity into Ure2p by point mutation

Ure2p, or its GST-like C-terminal domain (Ure2p-CTD), does not show typical GST activity towards the standard substrate CDNB.¹⁶ However, when we tested the ability of the series of G-site mutants described above to conjugate GSH to CDNB, a significant level of activity was detected for the point mutants A122C, N124A, and N124V (Fig. 1a). The other G-site mutants mentioned above were like WT Ure2p, in that they showed a negligible or only a very low level of GST activity (Fig. 1a and data not shown). In particular, although the residue equivalent to Asn124 in other known GSTs is Ser, Tyr or

Cys,^{3,5} the mutants N124S, N124Y and N124C all had a low level of, or negligible, GST activity, despite the fact that N124S showed a level of GPx activity similar to that of the WT (Fig. 1a). Further, the side chain of Arg164 makes van der Waals contacts and is hydrogen-bonded to the backbone atoms of GSH,¹⁰ and the corresponding residue is Asn or Gln in bacterial or eukaryotic GSTs.^{10,20} However, R164Q showed no GST activity towards CDNB (data not shown), while also showing a very low level of GPx activity (Fig. 1c). These results suggest that the environment of the G-site cleft of Ure2p may differ from that of other GSTs.

Comparison of WT (or N124S) with the mutants N124A and N124V suggests that in the case of the 124-site mutants of Ure2p, a gain in the level of GST activity is accompanied by a loss in the level of GPx activity (Fig. 1a). This implies that different substrate positioning may be required for the two types of activity in Ure2p. Although mutants A122C and N124A each showed a measurable level of both GPx and GST activity, the double mutant A122C/N124A showed reduced levels of both activities (Fig. 1a), suggesting disruption of the active site, although the overall secondary structure was unchanged compared to that of the WT (Fig. 1b).

Purification of the mutant A122C was initially carried out in a manner identical with that of the other mutants; i.e. in the absence of DTT (designated A122C-ox here). It was found subsequently that treatment with DTT during purification resulted in an increased level of GST activity (Fig. 1a), suggesting that a proportion of the A122C-ox protein is inactive due to masking of the free thiol group; however, in other respects the properties of A122C and A122C-ox are the same (see below).

The GST activity of Ure2p-CTD mutants was at least as high as that for the corresponding full-length mutants (Fig. 1a), indicating that the N-terminal prion domain of Ure2p does not contribute to the GST activity and may even interfere with substrate binding (see below). We therefore used the Ure2p-CTD mutants for further characterization of the GST activity.

Characterization of the GST activity of the Ure2p mutants

As expected for enzymatic activity, the initial velocities of the GST activity of the active Ure2p-CTD mutants A122C (or A122C-ox), N124A and N124V were found to be proportional to the concentration of enzyme (Fig. 2a), and substrate concentration dependence was observed in Michaelis-Menten plots (Fig. 2b and c).

The pH and temperature dependence of the GST activity for A122C (or A122C-ox) showed significant differences from that of the 124-site mutants N124A and N124V (Fig. 3). All three proteins showed a pH optimum of around 9, although the pH dependence of GST activity was more pronounced for the 124-site mutants (Fig. 3a). Conversely, the temperature dependence of the GST reaction was more pro-

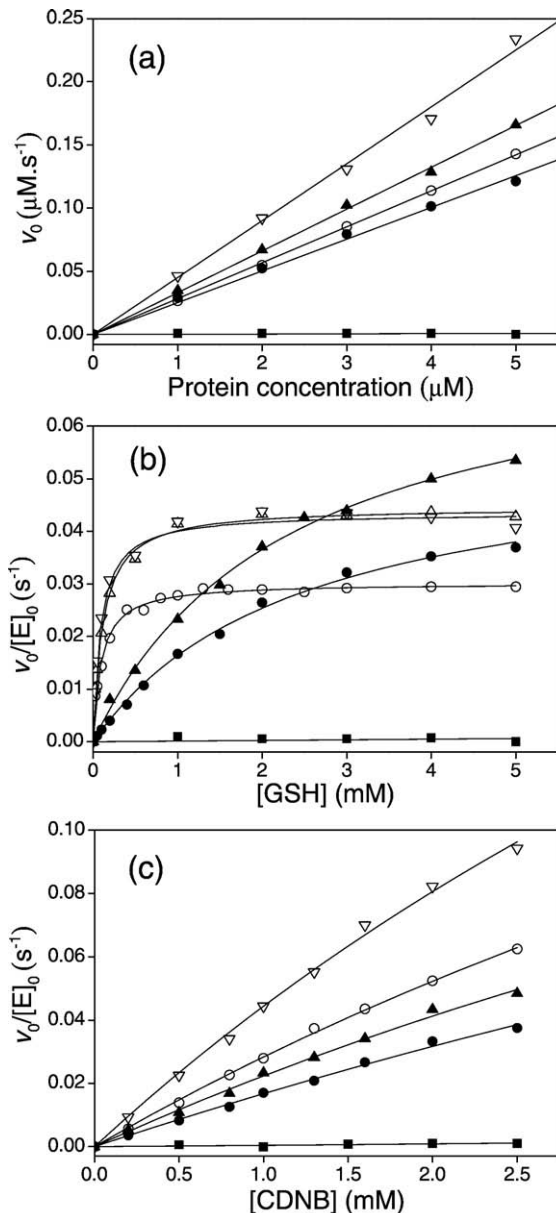


Fig. 2. Enzyme and substrate concentration dependence of the GST activity of Ure2p mutants. The proteins used were the Ure2p C-terminal domain (Ure2p-CTD, (■)) and its active mutants A122C (∇), A122C-ox (\circ), A122C-ox with 1 mM DTT (Δ), N124A (\bullet) and N124V (\blacktriangle). The reaction conditions were 100 mM sodium phosphate buffer, pH 7.5 at 25 °C. The protein concentration was 4 μM , and the CDNB and GSH concentrations were 1 mM, unless otherwise indicated. The baseline measured in the absence of enzyme was subtracted in each case. (a) Protein concentration dependence of the GST activity of Ure2p mutants. The GSH concentration was 1 mM for A122C and A122C-ox; but 2 mM for N124A, N124V and WT Ure2p-CTD. (b) and (c) Michaelis-Menten plots showing the substrate concentration dependence of the GST activity of Ure2p mutants at a fixed concentration of one substrate and varying concentrations of the other. Note that the maximum CDNB concentration is limited by the solubility of this substrate.

nounced for the A122C mutant (Fig. 3b). The optimum temperature for the 124-site mutants was about 30 °C, while that for A122C (or A122C-ox) was shifted to about 42 °C. The uncatalyzed velocity was observed to increase dramatically above pH 8.0 and 35 °C. Therefore, we chose pH 7.5 and 25 °C as the standard conditions for the GST activity assay for all mutants.

WT Ure2p or Ure2p-CTD, as controls, showed no detectable GST activity under the conditions used (Figs. 1a, 2 and 3).

Steady-state kinetic analysis of the GST activity of Ure2p mutants

Apparent kinetic parameters for the GST activity of Ure2p-CTD mutants were obtained from Michaelis-Menten plots (Fig. 2b and c) and are shown in Table 1. When the concentration of one substrate was fixed and the concentration of the other substrate was varied, the GST activity was hyperbolic with respect to the concentration of the first substrate and double-reciprocal plots were linear (Figs. 2b and c, and 4). The mutants N124A and N124V had apparent kinetic parameters different from those of A122C (or A122C-ox), particularly in terms of the K_m for GSH (Fig. 2b; Table 1).

In general, the activity of Ure2p-CTD mutants was the same or slightly higher than that of the equivalent full-length mutants (Fig. 1a; Table 1). The apparent $K_{m(\text{GSH})}$ value of full-length A122C was ~ 5 -fold higher than that of the equivalent CTD mutant, but the k_{cat} value was the same within experimental error (Table 1). It is possible that the presence of the N-terminal prion domain interferes with binding of GSH in the active site. However, there was no significant effect on the $K_{m(\text{GSH})}$ values for N124A or N124V, which are at least fivefold higher than the $K_{m(\text{GSH})}$ for A122C (Tables 1 and 3). This indicates that any effect of the prion domain on activity is minor, and its manifestation may depend on the orientation and affinity of binding (and/or the reaction mechanism, see below).

Investigation of the GST reaction mechanisms for A122C versus 124-site mutants

The initial velocity of GSH conjugation to CDNB was determined as a function of substrate concentration by varying the concentration of one substrate while the concentration of the other substrate was kept constant. Double-reciprocal plots at different fixed concentrations of GSH and CDNB show straight lines and allow extrapolation to obtain true kinetic parameters. All the data were fit globally to the Dalziel equation:

$$\frac{[E]_0}{v_0} = \Phi + \frac{\Phi_{\text{GSH}}}{[\text{GSH}]_0} + \frac{\Phi_{\text{CDNB}}}{[\text{CDNB}]_0} + \frac{\Phi_{\text{GSH-CDNB}}}{[\text{GSH}]_0[\text{CDNB}]_0} \quad (1)$$

in which v_0 is the initial velocity of the reaction, $[E]_0$ is the total concentration of the Ure2p variants,

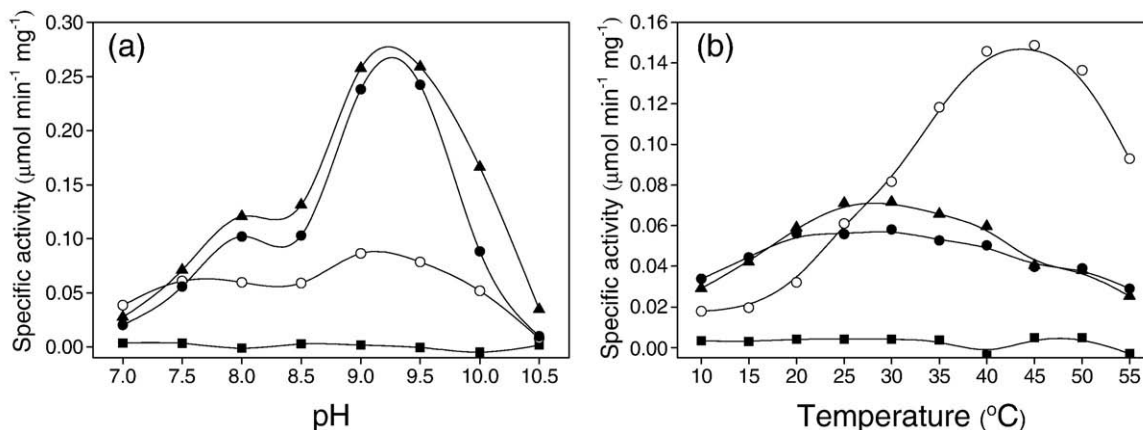


Fig. 3. Effects of temperature and pH on the GST activity of Ure2p mutants. The proteins used were the Ure2-CTD (■) and its active mutants A122C-ox (○), N124A (●) and N124V (▲). The reaction conditions were 100 mM phosphate buffer (pH 7.0–8.5), 100 mM bicine buffer (pH 9.0) or 100 mM sodium carbonate/sodium bicarbonate buffer (pH 9.5–10.5), with 2 mM GSH and 1 mM CDNB. (a) pH dependence, measured at 25 °C. (b) Temperature dependence, measured at pH 7.5. A122C shows the same pattern of temperature dependence as A122C-ox (data not shown).

and Φ_0 , Φ_{GSH} , Φ_{CDNB} , $\Phi_{\text{GSH-CDNB}}$ are the Dalziel parameters and are shown in Table 2. The true kinetic parameters calculated from the Dalziel parameters for the three Ure2p-CTD mutants A122C, N124A and N124V are shown in Table 3.

The results for A122C show two sets of parallel lines (Fig. 4a and b), suggesting a ping-pong mechanism. Groups of intersecting straight lines were observed in the assays for N124V (Fig. 4c and d) and N124A (data not shown), suggesting a sequential mechanism for these mutants.

There are, of course, some conditions where converging reciprocal lines will appear parallel.²¹

Further, the low level of solubility of the substrates, particularly CDNB, means that saturating conditions cannot be attained. Therefore, we cannot prove definitively from the data that the mutant A122C has a ping-pong mechanism. However, it is clear that the kinetic behavior of A122C is distinctly different from that of the 124-site mutants.

Importance of the free thiol group for GST activity of A122C

We observed that treatment with DTT during purification (and subsequent removal of the DTT by

Table 1. Apparent steady-state kinetic parameters for Ure2p mutants that show GST activity

Protein	Fixed [CDNB] at 1.0 mM		Fixed [GSH] at 1.0 mM	
	$K_{\text{m(GSH)}}(\text{app})$ (mM)	$V_{\text{max}}(\text{app})/[\text{E}]_0$ (s ⁻¹)	$K_{\text{m(CDNB)}}(\text{app})$ (mM)	$V_{\text{max}}(\text{app})/[\text{E}]_0$ (s ⁻¹)
A. Full-length Ure2p mutant				
Without DTT				
A122C	0.48±0.05	0.042±0.001	ND	ND
A122C-ox	0.40±0.06	0.019±0.003	ND	ND
N124A	2.6±0.3	0.035±0.003	ND	ND
N124V	1.7±0.2	0.057±0.003	ND	ND
B. Ure2p-CTD mutant				
Without DTT				
A122C	0.09±0.01	0.044±0.001	8.6±1.4	0.43±0.08
A122C-ox	0.10±0.01	0.029±0.001	8.2±2.4	0.29±0.06
N124A	2.3±0.4	0.050±0.005	16.6±8.1	0.29±0.13
N124V	2.1±0.2	0.063±0.006	11.5±1.1	0.30±0.09
With 1 mM DTT				
A122C	0.10±0.01	0.045±0.002	ND	ND
A122C-ox	0.11±0.01	0.045±0.002	ND	ND
N124A	2.1±0.4	0.053±0.006	ND	ND
N124V	2.0±0.3	0.065±0.005	ND	ND

The apparent kinetic parameters were determined from Michaelis-Menten plots of initial velocities at various concentrations of one substrate with a fixed concentration of the other substrate, as shown in Fig. 2b and c. The concentration of CDNB was fixed at 1 mM, while the GSH concentration was varied from 0.02 mM to 5 mM. Alternatively, the GSH concentration was fixed at 1 mM while the CDNB concentration was varied from 0.2 mM to 2.5 mM. The concentrations of Ure2p mutants were 4.0–5.0 μM. Other conditions are as described in the legend to Fig. 2. The A122C mutant protein purified in the absence of DTT is indicated as A122C-ox. ND, not determined. The values shown are the mean±S.E. of at least three repeated measurements.

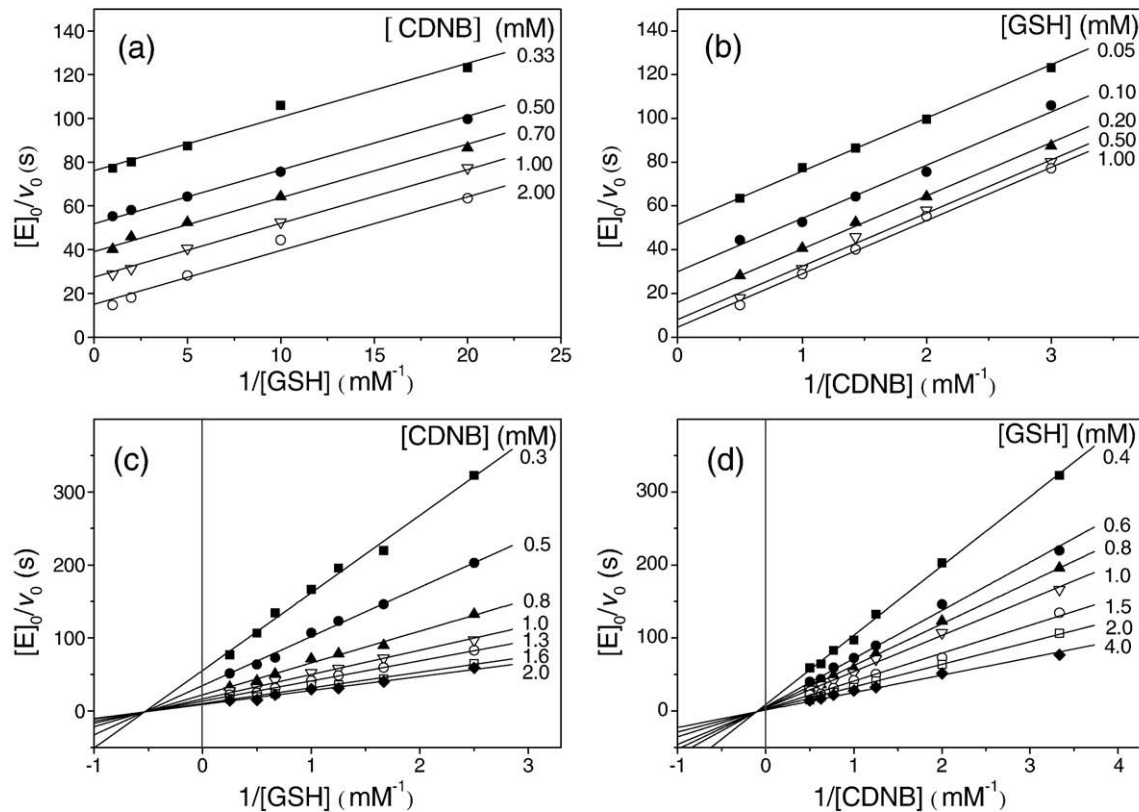


Fig. 4. Difference in the kinetic mechanism of the GST activity for 122-site and 124-site mutants of Ure2p. Double-reciprocal plots show the pattern of substrate concentration dependence when the concentration of one substrate (GSH or CDNB) is fixed and the other is varied. Parallel lines suggest a ping-pong mechanism, whereas converging lines indicate a sequential mechanism. The parameters obtained by global fitting of the data to the Dalziel equation are shown in Table 2. (a) and (b) Ure2p-CTD mutant A122C assayed in the presence of 1 mM DTT. (The results for A122C measured in the absence of DTT showed the same pattern and the true kinetic parameters obtained were the same within error, data not shown.) The protein concentration was 8.0 μ M. (c) and (d) Ure2p-CTD mutant N124V. (The pattern observed for N124V was the same.) The protein concentration was 4.4 μ M.

dialysis) significantly increased the apparent GST activity of the A122C mutants, compared to A122C that was purified without DTT (A122C-ox); whereas the effect on the GPx activity was less significant (Fig. 1a). This suggests strongly that the free thiol group is involved in the GST activity of A122C. The apparent k_{cat} value for A122C-ox was lower than for

Table 2. Dalziel parameters for the GST activity of the Ure2p-CTD mutants A122C, N124A and N124V derived from steady-state kinetic analysis

Ure2p-CTD mutant	Dalziel parameters			
	Φ_0	Φ_{GSH}	Φ_{CDNB}	$\Phi_{\text{GSH-CDNB}}$
	(s)	(mM s)	(mM s)	(mM ² s)
A122C (1 mM DTT)	3.4 \pm 0.7	2.46 \pm 0.06	24.3 \pm 0.4	—
N124A	0.7 \pm 0.1	2.32 \pm 0.07	16.8 \pm 1.9	46.6 \pm 1.4
N124V	0.6 \pm 0.1	3.3 \pm 0.1	16.7 \pm 1.3	31.1 \pm 1.0

The kinetic parameters were determined using [A122C]=8.0 μ M, [N124A]=4.0 μ M and [N124V]=4.4 μ M; [GSH]=0.1–1.0 mM, [CDNB]=0.5–2.0 mM for A122C; [GSH]=0.4–4.0 mM, [CDNB]=0.3–2.0 mM for N124A and N124V to obtain a series of sets of data as shown in Fig. 4 (and data not shown). The parameters were obtained by global fitting of the data to the Dalziel equation. The errors shown are the standard error of the fit.

A122C, but full activity could be restored by inclusion of DTT in the enzyme assay buffer (Table 1). The apparent $K_{\text{m}(\text{GSH})}$ for A122C-ox and A122C were identical (Fig. 2b), and the presence or absence of DTT in the assay buffer had no effect on any of the kinetic parameters for A122C, N124A or N124V (Table 1) or on the apparent reaction mechanism for A122C (Fig. 4a and b, and data not shown). This indicates that the DTT molecule itself does not contribute to the reaction. These results suggest that a proportion of the A122C-ox protein has lost its GST activity due to oxidation of the Cys residue, such as by disulphide bond formation with another Ure2 molecule. Consistent with this, examination of A122C-ox by non-reducing SDS-PAGE shows the presence of a major band at the size expected for the monomer and a minor band at the size expected for a dimer (data not shown).

Using Ure2p-CTD, we found that A122C showed no GST activity after modification of the thiol group with iodoacetic acid, whereas N124A and N124V retained almost the same level of GST activity after this treatment (Fig. 5). This confirms that it is the thiol group in A122C that has an essential role in GST activity. The number of free thiol groups in each molecule of A122C determined using DTNB

Table 3. True kinetic parameters for the GST activity of Ure2p-CTD mutants

Kinetic parameter	Ure2p-CTD Mutant			Method of calculation
	A122C (1 mM DTT)	N124A	N124V	
k_{cat} (s^{-1})	0.30 ± 0.06	1.4 ± 0.2	1.7 ± 0.3	$1/\Phi_0$
$K_{\text{m(GSH)}}$ (mM)	0.7 ± 0.1	3.3 ± 0.3	5.8 ± 1.4	Φ_{GSH}/Φ_0
$K_{\text{m(CDNB)}}$ (mM)	7.2 ± 1.4	23.8 ± 4.8	29.2 ± 7.3	$\Phi_{\text{CDNB}}/\Phi_0$
$K_{\text{t}}^{\text{CDNB}}$ (mM)	–	20.1 ± 0.8	9.4 ± 0.4	$\Phi_{\text{CDNB-GSH}}/\Phi_{\text{GSH}}$
$K_{\text{t}}^{\text{GSH}}$ (mM)	–	2.8 ± 0.1	1.9 ± 0.1	$\Phi_{\text{CDNB-GSH}}/\Phi_{\text{CDNB}}$
$k_{\text{cat}}/K_{\text{m(GSH)}}$ ($\text{M}^{-1}\text{s}^{-1}$)	410 ± 10	430 ± 10	300 ± 10	$1/\Phi_{\text{GSH}}$
$k_{\text{cat}}/K_{\text{m(CDNB)}}$ ($\text{M}^{-1}\text{s}^{-1}$)	41 ± 1	60 ± 7	60 ± 5	$1/\Phi_{\text{CDNB}}$

The kinetic parameters were calculated from the Dalziel parameters shown in Table 2, in the manner indicated. The errors shown are derived from the standard error of the fit, as shown in Table 2.

was 1.0 before modification and 0.2 afterwards, which correlates with the presence or absence of GST activity.

GST activity is maintained in amyloid-like fibrils of mutant Ure2p

The sigmoidal time course for formation of amyloid-like fibrils of Ure2p monitored using the fluorescent dye Thioflavin T (ThT)^{13,17,22} under the GST assay conditions is shown in Fig. 6a. To avoid any complication of the presence of a free thiol group, the mutants N124A and N124V were used in this experiment. Fibrils of full-length N124V Ure2p (Fig. 6b) and N124A Ure2p (data not shown) maintained a significant level of GST activity, indicating that fibril formation has little effect on the GST activity of Ure2p mutants. This is consistent with the observation of GPx activity in both WT Ure2p fibrils *in vitro*,¹⁷ and the prion state *in vivo*,¹⁵ and indicates maintenance of native-like structure in the C-terminal GST-like domain within the Ure2p fibrils.

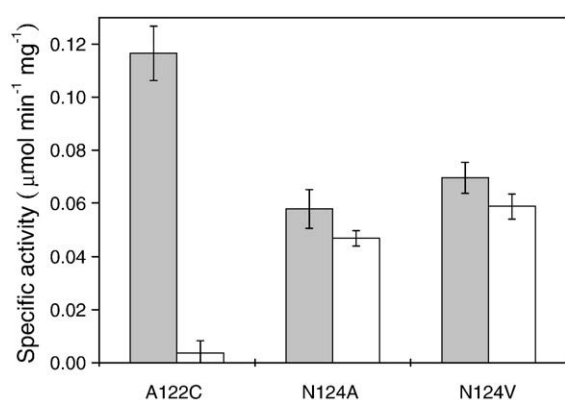


Fig. 5. Comparison of GST activity of Ure2p mutants before and after iodoacetic acid treatment. Mutants of Ure2p-CTD were used, as indicated. Iodoacetic acid modification was carried out to block free thiol groups. GST activity before (filled bars) and after (open bars) modification is shown. The reaction conditions were 25 °C in 100 mM sodium phosphate buffer, pH 7.5 containing 2 mM GSH, 1 mM CDNB, 1 mM EDTA, and 1 mM DTT. The protein concentration was 5.0 μM . The error bars represent the standard error of at least three repeated measurements.

Discussion

The yeast prion protein Ure2p, while showing clear similarity to the GST enzyme family in both sequence and structure, has presented a paradox for many years by its lack of typical GST activity, such as conjugation of GSH to the compound CDNB. A key step in GST activity is the activation of GSH, which typically involves interaction of the polar side chain of Ser or Tyr (or Cys in a few bacterial examples) with the thiol group of GSH, thought to result in formation of a thiolate ion.¹ The observation that the residue equivalent to the catalytic Ser or Tyr appears to be Ala122^{9,23} or Asn124¹⁰ in Ure2p initially presented an explanation for its apparent lack of catalytic activity, and suggested that Ure2p, like many bacterial members of the GST-structural family,² might have adapted the GST-fold to serve a very different function. However, the finding that Ure2p does in fact display the ability to catalyze the conjugation of GSH to hydroperoxide substrates, indicating GPx-like activity,^{15,17} presented the paradox once again.

Here, we demonstrate that Asn124 indeed has a key role in the catalytic mechanism of the GPx activity of Ure2p. Further, mutation of either Ala122 or Asn124 can "restore" GST activity to Ure2p. The mutant N124S was found to have GPx activity similar to that of WT Ure2p, suggesting that Asn124 might function in a way similar to that of the catalytic Ser of typical GST enzymes in activation of GSH. However, N124S did not show GST activity and, in general, restoration of GST activity by point mutation of Ala122 or Asn124 coincided with reduction in the native GPx activity of Ure2p.

Many enzymes show cross-reactivity with related substrates.^{24,25} The observation that a number of GST enzymes also show GPx activity^{2,26} would seem to be a good example of this, as the same reducing agent (GSH) is conjugated to a second substrate to lower its toxicity. Further, the second substrate, which might be an organic compound containing an electrophilic group (in the case of GST activity) or an organic hydroperoxide (in the case of GPx activity), might well be expected to bind in a similar way within the active site of the enzyme. In addition to binding different substrates in a similar way, cross-reactivity is expected to involve similar

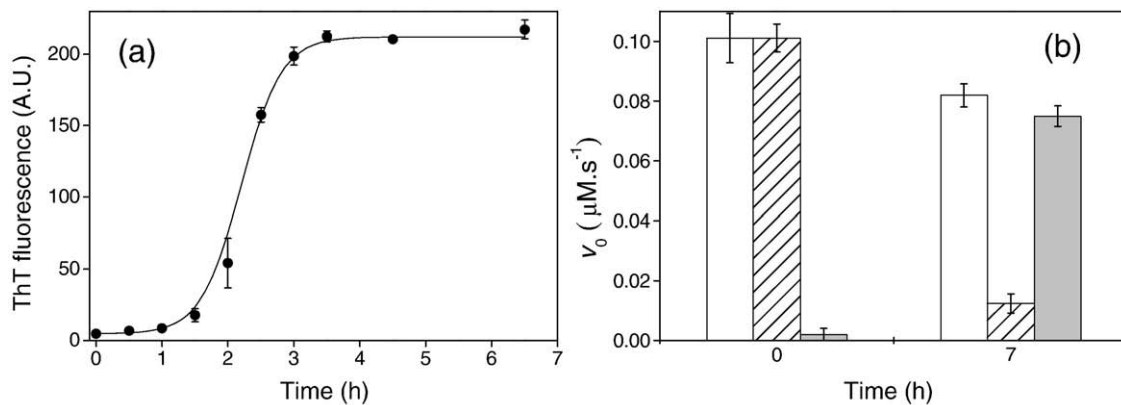


Fig. 6. GST activity is maintained within amyloid-like fibrils of Ure2p. Full-length N124V Ure2p was used. (The results for N124A were similar.) Fibril formation was performed in 50 mM Tris-HCl, pH 8.4, 0.2 M NaCl at 30 °C with shaking. The protein concentration was 50 μM . (a) Fibril formation was monitored by assaying the change in ThT fluorescence. (b) GST activity in the total reaction mixture (open bars), supernatant fraction (hatched bars), and pellet fraction (filled bars) at the zero time point and plateau phase end point shown in a. The initial velocities are shown for a final protein concentration in the GST assay of 5.0 μM for the total reaction mixture and a maximum of 5.0 μM in either the pellet or the supernatant fractions. The error bars represent the standard error of at least three repeated measurements.

catalytic mechanisms. Consistent with this, the observed substrate dependence of the steady-state kinetics for the GPx activity of WT Ure2p is consistent with a sequential mechanism (i.e., both substrates must bind before products are released), as is typically observed for the GST activity of other related enzymes.^{17,27} The GST activity of Ure2p mutants N124A and N124V likewise shows a sequential mechanism. However, mutations that increase GST activity appear to cause a proportional decrease in GPx activity, which suggests that if the mechanisms are similar, then at least the optimal substrate positioning for the two activities is different. Another surprising finding is that N124A/V lacks any obvious polar residue to allow activation of GSH for either GST or GPx activity. However, it is possible that these mutants allow accommodation of a water molecule within the active site, which may then function in this role. Another possible explanation is that mutation of the Asn124 side chain to Ala or Val allows binding and orientation of GSH and CDNB in a manner that allows catalysis by a proximity effect. A similar example was reported by Jahn *et al.*, in which the exchange of two polar Glu residues for non-polar Ala and Gly in the active site of a glycosidase allowed thioglycosynthase activity, although the double mutant lacks the original glycosidase activity.²⁸

In addition to cross-reactivity, another concept that has relevance to the findings of this study is promiscuity (or substrate ambiguity) of enzyme activity.^{25,29} One view of the evolutionary origin of present day enzyme specificity and activity is that progenitor enzymes were generalists, with a broad spectrum of low-level activities. These primordial enzymes then evolved to have much higher specificity and activity for a single function, but some of the low-level generalist functions were retained.

Promiscuous activities share the same active site and generally show a similar mechanism, although differences in substrate positioning, and even differences in catalytic residues, may be observed.³⁰ The single mutations A122C and N124A each allows the concomitant existence of detectable levels of GPx and GST activity in Ure2p. However, the double mutant A122C/N124A shows negligible levels of either activity. This supports the idea that different substrate positioning is required for the GPx and GST activities of Ure2p, and/or that Asn124 contributes to the GST activity of A122C. More interesting is the fact that the GST activity of A122C shows steady-state kinetics distinctly different from that of the 124-site mutants, and shows parallel lines in double reciprocal plots, suggesting that the reaction may occur via a ping-pong mechanism (i.e., where the first substrate reacts to form a covalent intermediate and the first product is released, before reaction of the second substrate). The mutant A122S showed reduced GPx activity and only a very low level of GST activity, consistent with the participation of the free thiol group of A122C in the GST reaction mechanism. Adherence to a ping-pong mechanism is challenging to prove definitively, as converging lines may appear parallel, particularly where the range of substrate concentrations that can be tested is limited by solubility, which is the case here. However, the possibility of a ping-pong mechanism for the GST activity of A122C is consistent with the reaction mechanism of classical GPx enzymes, which typically have selenocysteine as the key catalytic residue.^{31,32} The selenocysteine-containing GPx family, like the GST structural family, contains a thioredoxin-like domain, and they are suggested to have evolved from a common ancestor,³³ although the GPx (EC 1.11.1.9) and GST (EC 2.5.1.18) structural classes are considered to be distinct enzyme families. There are

a number of examples in nature where members of the same enzyme superfamily use similar structures to catalyze different types of reaction; the observation of residual levels of the alternative activity supports the idea of divergent evolution of enzymes from a common progenitor by gene duplication and selection for specific activities.³⁴

The results of this study provide insight into how Ure2p and other GST-like or GPx-like enzymes may have originated from an ancient thioredoxin-like enzyme, which harbored a range of low-level activities allowing it to couple the tripeptide GSH to a variety of secondary substrates to reduce their toxicity. The finding that point mutations can restore the GST activity of Ure2p supports the idea that mutation of one or a few plasticity residues can bring about dramatic increases in promiscuous activities and a switch in substrate specificity.^{30,35,36} This is then consistent with the diverse range of activities observed in nature that are associated with the thioredoxin-like fold in general, and GST-structural family in particular, especially in rapidly evolving microorganisms, such as bacteria. Ure2p contains an unstructured N-terminal prion domain (residues 1–93); and a flexible α -cap region (residues 267–298), suggested to be important for the interaction with partner proteins.^{8,10} Bioinformatics analysis shows these two additional regions, which are absent from other members of the GST structural family, emerged at the same time in many kinds of yeasts, but the N-terminal region has diverged faster than the GST-like region.³⁷ Clearly, mechanisms such as domain addition or insertion^{5,38} have allowed Ure2p to diversify and acquire additional functions as a prion and a repressor of nitrogen catabolism. However, this study demonstrates that Ure2p still harbors characteristics of an ancient glutathione transferase progenitor.

Materials and Methods

Mutagenesis and heterologous protein expression

The URE2 mutants were constructed by PCR-based, site-directed mutagenesis with a WT synthetic URE2 gene as template.¹⁹ All mutations were verified by DNA sequencing. All proteins were expressed in *Escherichia coli* with a short N-terminal His₆ tag to allow a high level of purity to be achieved. WT Ure2p and full-length Ure2p point mutants were purified under native conditions by nickel chromatography as described,¹⁹ except that a French press was used to disrupt the cells instead of sonication. Full-length proteins were stored at -80°C in 50 mM Tris-HCl buffer, pH 8.4, 0.2 M NaCl. Ure2p-CTD lacks the entire N-terminal unstructured region and contains only the C-terminal domain (CTD) of Ure2p (residues 105–354). The stability and folding of Ure2p-CTD is identical with that of the WT.³⁹ For the purification of Ure2p-CTD with and without point mutations, *E. coli* cells expressing the corresponding gene were harvested and resuspended in 20 mM Tris-HCl buffer, pH 8.4. Cells were then lysed using a French press and the supernatant of the *E. coli* extract was purified by nickel chromato-

graphy, after which the proteins eluted from the column were dialyzed against 10 mM Tris-HCl buffer, pH 8.4 or pH 7.5, to remove imidazole and then stored at -80°C . The A122C mutants of full-length Ure2p and Ure2p-CTD (including A122C/N124A) were purified as described above, except that after elution from the nickel affinity resin, 2 mM DTT was added to the initial dialysis buffer, and then the DTT was removed by subsequent dialysis. (A122C purified in the absence of DTT, designated here as A122C-ox, was found to have reduced activity, unless subsequently treated with DTT; see Results.) All the proteins were purified to $>98\%$ purity as judged by SDS-PAGE. Proteins were thawed in a 25°C water bath immediately before use. Monomeric protein concentrations were determined by measuring the absorbance at 280 nm and using the calculated extinction coefficient of $48,200\text{ M}^{-1}\text{cm}^{-1}$.^{19,40}

Circular dichroism

Circular dichroism spectra were measured over the range 200–260 nm in a Pistar-180 spectrometer (Applied Photophysics, UK). Measurements were made at 25°C in a 0.1 mm path-length thermostatically controlled cuvette after incubation for 10 min at 25°C . The conditions for full-length WT or mutant Ure2p were 40 μM protein in 50 mM Tris-HCl, pH 8.4, 0.2 M NaCl. For Ure2p-CTD and its mutants, the conditions were 50 μM protein in 10 mM Tris-HCl, pH 8.4.

Assay of enzymatic activity

Measurements of enzymatic activity were done at 25°C using a Shimadzu UV2501 spectrophotometer. The GPx activity of Ure2p and its variants was determined using GSH and CHP as substrates in a spectrometric coupled assay as described.^{17,41} The reaction was carried out in 1 ml of 100 mM sodium phosphate buffer, pH 7.5, containing 1 mM GSH, 0.15 mM β -NADPH, 0.24 unit of glutathione reductase and 1.0–3.0 μM WT or mutant Ure2p. The mixture was preincubated at 25°C for 6 min. The CHP was then added to the cuvette to a final concentration of 1.2 mM to trigger the reaction. The activity was measured from the continuous decrease of β -NADPH absorption at 340 nm for 5 min. All initial velocities were corrected by subtraction of the non-enzymatic reaction measured using an equivalent volume of buffer in place of the protein solution.

The GST activity toward CDNB of Ure2p variants was measured spectrophotometrically essentially as described,⁴² in a 1 ml reaction volume containing 100 mM sodium phosphate buffer, pH 7.5, 0.02–5.0 mM GSH, 0.2–2.5 mM CDNB and 1.0–5.0 μM protein, at 25°C . The rate was observed by measuring the continuous increase in the absorbance at 340 nm for about 120 s. The initial velocity of the reaction was calculated from the slope of the linear region of the progress curve using an extinction coefficient for production of S-(2,4-dinitrophenyl)-glutathione of $9600\text{ M}^{-1}\text{cm}^{-1}$, after subtraction of the velocity of the non-enzymatic reaction measured using an equivalent volume of buffer in place of the protein solution.

Steady-state kinetic analysis

The initial velocity was measured over a wide range of concentrations of one substrate and a fixed concentration of the other substrate. The data were fit to the Michaelis-

Menten, Lineweaver-Burk and Eadie-Hofstee equations. The values obtained from these plots were the same within experimental error.

The true kinetic parameters and the reaction mechanisms of Ure2p-CTD containing point mutations were determined from a family of double-reciprocal plots at various concentrations of substrate. The data were fit globally to the Dalziel equations describing the reaction mechanisms for two substrates.

Modification of thiol-containing Ure2p mutant

Modification of the thiol group of Ure2p-CTD containing the mutation A122C was performed using 15 mM iodoacetic acid, as described.⁴³ The number of free thiol groups before and after modification was determined using DTNB, as described.^{43,44} The GST activity assay using 2 mM GSH, 1 mM CDNB, 1 mM EDTA, 1 mM DTT and 5 μ M protein in 100 mM sodium phosphate buffer, pH 7.5, was performed as described above, both before and after modification. Ure2p-CTD mutants N124A and N124V were used as controls and were subjected to the experimental procedures described above.

Assay of GST activity of Ure2p mutants during amyloid-like fibril formation

The effect of fibril formation on the GST activity of Ure2p mutants was assayed essentially as described for the assay of GPx activity during fibril formation of Ure2p.¹⁷ The initial protein solution was centrifuged at 18,000g for 25 min at 4 °C to remove any pre-existing aggregates, then 400 μ l of the supernatant was transferred to a tube containing a bead. The sample for formation of amyloid-like fibrils contained 50 μ M full-length Ure2p mutants in 50 mM Tris-HCl, pH 8.4, 0.2 M NaCl. The samples were incubated at a constant temperature of 30 °C with shaking as described.^{13,22} The time course of fibril formation was monitored by ThT binding fluorescence. When the plateau phase was reached, a 100 μ l aliquot of complete reaction mixture containing fibrils was removed and assayed for GST activity using 1 mM GSH and 1 mM CDNB as substrates, as described above. Another identical 100 μ l aliquot of complete reaction mixture was centrifuged at 18,000g for 25 min at 4 °C to separate the fibril pellet and supernatant fractions. The pellet was resuspended in 100 μ l of the same buffer. Both the resuspended pellet and supernatant were assayed for GST activity as described above. The non-enzymatic reaction baseline was subtracted in each case. As a control, the zero time-point protein sample was centrifuged and assayed for GST activity as described above.

Acknowledgements

We thank Professor Zhixin Wang for helpful comments on the manuscript. This work was supported by grants from the National Natural Science Foundation of China (30470363, 30620130109, 30670428), the Chinese Ministry of Science and Technology (2006CB500703, 2006CB910903) and the Chinese Academy of Sciences (KSCX2-YW-R-119).

References

1. Armstrong, R. N. (1997). Structure, catalytic mechanism, and evolution of the glutathione transferases 45. *Chem. Res. Toxicol.* **10**, 2–18.
2. Vuilleumier, S. (1997). Bacterial glutathione S-transferases: what are they good for? *J. Bacteriol.* **179**, 1431–1441.
3. Sheehan, D., Meade, G., Foley, V. M. & Dowd, C. A. (2001). Structure, function and evolution of glutathione transferases: implications for classification of non-mammalian members of an ancient enzyme superfamily. *Biochem. J.* **360**, 1–16.
4. Hayes, J. D., Flanagan, J. U. & Jowsey, I. R. (2005). Glutathione transferases. *Annu. Rev. Pharmacol. Toxicol.* **45**, 51–88.
5. Oakley, A. J. (2005). Glutathione transferases: new functions. *Curr. Opin. Struct. Biol.* **15**, 716–723.
6. Wickner, R. B. (1994). [URE3] as an altered URE2 protein: evidence for a prion analog in *Saccharomyces cerevisiae*. *Science*, **264**, 566–569.
7. Masison, D. C. & Wickner, R. B. (1995). Prion-inducing domain of yeast Ure2p and protease resistance of Ure2p in prion-containing cells. *Science*, **270**, 93–95.
8. Bousset, L., Belrhali, H., Janin, J., Melki, R. & Morera, S. (2001). Structure of the globular region of the prion protein Ure2 from the yeast *Saccharomyces cerevisiae*. *Structure*, **9**, 39–46.
9. Umland, T. C., Taylor, K. L., Rhee, S., Wickner, R. B. & Davies, D. R. (2001). The crystal structure of the nitrogen regulation fragment of the yeast prion protein Ure2p. *Proc. Natl Acad. Sci. USA*, **98**, 1459–1464.
10. Bousset, L., Belrhali, H., Melki, R. & Morera, S. (2001). Crystal structures of the yeast prion Ure2p functional region in complex with glutathione and related compounds. *Biochemistry*, **40**, 13564–13573.
11. Taylor, K. L., Cheng, N., Williams, R. W., Steven, A. C. & Wickner, R. B. (1999). Prion domain initiation of amyloid formation in vitro from native Ure2p. *Science*, **283**, 1339–1343.
12. Thual, C., Bousset, L., Komar, A. A., Walter, S., Buchner, J., Cullin, C. & Melki, R. (2001). Stability, folding, dimerization, and assembly properties of the yeast prion Ure2p. *Biochemistry*, **40**, 1764–1773.
13. Jiang, Y., Li, H., Zhu, L., Zhou, J. M. & Perrett, S. (2004). Amyloid nucleation and hierarchical assembly of Ure2p fibrils. Role of asparagine/glutamine repeat and nonrepeat regions of the prion domains. *J Biol. Chem.* **279**, 3361–3369.
14. Lacroute, F. (1971). Non-Mendelian mutation allowing ureidosuccinic acid uptake in yeast. *J Bacteriol.* **106**, 519–522.
15. Rai, R., Tate, J. J. & Cooper, T. G. (2003). Ure2, a prion precursor with homology to glutathione S-transferase, protects *Saccharomyces cerevisiae* cells from heavy metal ion and oxidant toxicity. *J Biol. Chem.* **278**, 12826–12833.
16. Coschigano, P. W. & Magasanik, B. (1991). The URE2 gene product of *Saccharomyces cerevisiae* plays an important role in the cellular response to the nitrogen source and has homology to glutathione S-transferases. *Mol. Cell Biol.* **11**, 822–832.
17. Bai, M., Zhou, J. M. & Perrett, S. (2004). The yeast prion protein Ure2 shows glutathione peroxidase activity in both native and fibrillar forms. *J. Biol. Chem.* **279**, 50025–50030.
18. Choi, J. H., Lou, W. & Vancura, A. (1998). A novel membrane-bound glutathione S-transferase functions

- in the stationary phase of the yeast *Saccharomyces cerevisiae*. *J Biol. Chem.* **273**, 29915–29922.
19. Perrett, S., Freeman, S. J., Butler, P. J. & Fersht, A. R. (1999). Equilibrium folding properties of the yeast prion protein determinant Ure2. *J Mol. Biol.* **290**, 331–345.
 20. Nishida, M., Harada, S., Noguchi, S., Satow, Y., Inoue, H. & Takahashi, K. (1998). Three-dimensional structure of *Escherichia coli* glutathione S-transferase complexed with glutathione sulfonate: catalytic roles of Cys10 and His106. *J Mol. Biol.* **281**, 135–147.
 21. Segel, I. H. (1993). Enzyme kinetics: behavior and analysis of rapid equilibrium and steady state enzyme systems, pp. 623, Wiley, New York.
 22. Zhu, L., Zhang, X. J., Wang, L. Y., Zhou, J. M. & Perrett, S. (2003). Relationship between stability of folding intermediates and amyloid formation for the yeast prion Ure2p: a quantitative analysis of the effects of pH and buffer system. *J Mol. Biol.* **328**, 235–254.
 23. Rossjohn, J., Board, P. G., Parker, M. W. & Wilce, M. C. (1996). A structurally derived consensus pattern for theta class glutathione transferases. *Protein Eng.* **9**, 327–332.
 24. Copley, S. D. (2003). Enzymes with extra talents: moonlighting functions and catalytic promiscuity. *Curr. Opin. Chem. Biol.* **7**, 265–272.
 25. James, L. C. & Tawfik, D. S. (2003). Conformational diversity and protein evolution—a 60-year-old hypothesis revisited. *Trends Biochem. Sci.* **28**, 361–368.
 26. Mannervik, B. (1985). Glutathione peroxidase. *Methods Enzymol.* **113**, 490–495.
 27. Labrou, N. E., Mello, L. V. & Clonis, Y. D. (2001). Functional and structural roles of the glutathione-binding residues in maize (*Zea mays*) glutathione S-transferase I. *Biochem. J.* **358**, 101–110.
 28. Jahn, M., Chen, H., Mullegger, J., Marles, J., Warren, R. A. & Withers, S. G. (2004). Thioglycosynthases: double mutant glycosidases that serve as scaffolds for thioglycoside synthesis. *Chem. Commun. (Camb.)*, 274–275.
 29. Jensen, R. A. (1976). Enzyme recruitment in evolution of new function. *Annu. Rev. Microbiol.* **30**, 409–425.
 30. Khersonsky, O., Roodveldt, C. & Tawfik, D. S. (2006). Enzyme promiscuity: evolutionary and mechanistic aspects. *Curr. Opin. Chem. Biol.* **10**, 498–508.
 31. Ursini, F., Maiorino, M., Brigelius-Flohe, R., Aumann, K. D., Roveri, A., Schomburg, D. & Flohe, L. (1995). Diversity of glutathione peroxidases. *Methods Enzymol.* **252**, 38–53.
 32. Brigelius-Flohe, R. (1999). Tissue-specific functions of individual glutathione peroxidases. *Free Radic. Biol. Med.* **27**, 951–965.
 33. Martin, J. L. (1995). Thioredoxin—a fold for all reasons. *Structure*, **3**, 245–250.
 34. O'Brien, P. J. & Herschlag, D. (1999). Catalytic promiscuity and the evolution of new enzymatic activities. *Chem. Biol.* **6**, R91–R105.
 35. Schmidt, D. M., Mundorff, E. C., Dojka, M., Bermudez, E., Ness, J. E., Govindarajan, S. *et al.* (2003). Evolutionary potential of (beta/alpha)₈-barrels: functional promiscuity produced by single substitutions in the enolase superfamily. *Biochemistry*, **42**, 8387–8393.
 36. Varadarajan, N., Gam, J., Olsen, M. J., Georgiou, G. & Iverson, B. L. (2005). Engineering of protease variants exhibiting high catalytic activity and exquisite substrate selectivity. *Proc. Natl Acad. Sci. USA*, **102**, 6855–6860.
 37. Baudin-Baillieu, A., Fernandez-Bellot, E., Reine, F., Coissac, E. & Cullin, C. (2003). Conservation of the prion properties of Ure2p through evolution. *Mol. Biol. Cell*, **14**, 3449–3458.
 38. Ladner, J. E., Parsons, J. F., Rife, C. L., Gilliland, G. L. & Armstrong, R. N. (2004). Parallel evolutionary pathways for glutathione transferases: structure and mechanism of the mitochondrial class kappa enzyme rGSTK1-1. *Biochemistry*, **43**, 352–361.
 39. Lian, H. Y., Jiang, Y., Zhang, H., Jones, G. W. & Perrett, S. (2006). The yeast prion protein Ure2: structure, function and folding. *Biochim. Biophys. Acta*, **1764**, 535–545.
 40. Gill, S. C. & von Hippel, P. H. (1989). Calculation of protein extinction coefficients from amino acid sequence data. *Anal. Biochem.* **182**, 319–326.
 41. Flohe, L. & Gunzler, W. A. (1984). Assays of glutathione peroxidase. *Methods Enzymol.* **105**, 114–121.
 42. Habig, W. H. & Jakoby, W. B. (1981). Assays for differentiation of glutathione S-transferases. *Methods Enzymol.* **77**, 398–405.
 43. Quan, H., Fan, G. & Wang, C. C. (1995). Independence of the chaperone activity of protein disulfide isomerase from its thioredoxin-like active site. *J Biol. Chem.* **270**, 17078–17080.
 44. Ellman, G. L. (1959). Tissue sulfhydryl groups. *Arch. Biochem. Biophys.* **82**, 70–77.